Report

Cell Reports

Optineurin Negatively Regulates Osteoclast Differentiation by Modulating NF-κB and Interferon Signaling: Implications for Paget's Disease

Graphical Abstract

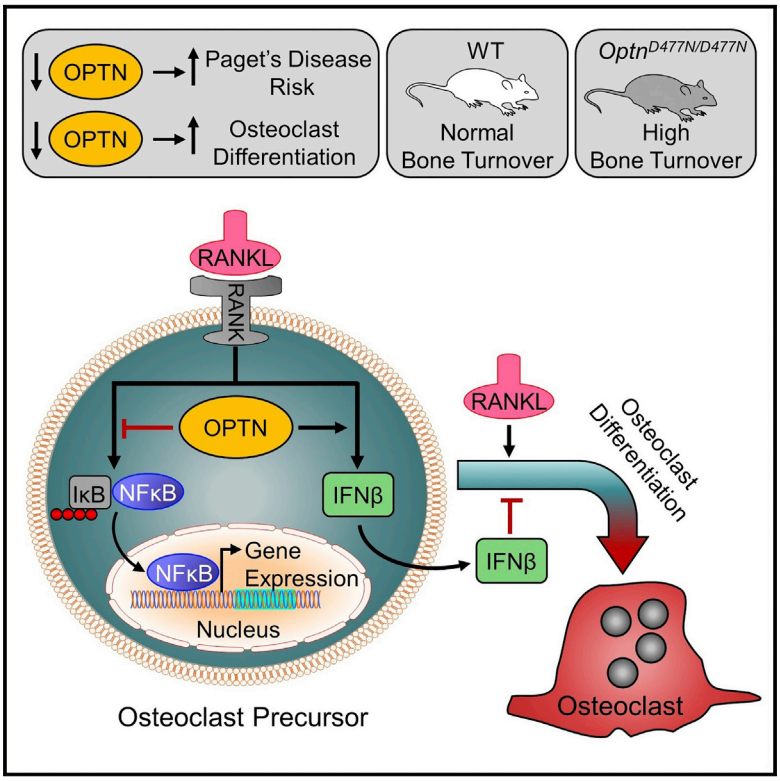

Highlights

- Susceptibility to Paget's disease is associated with reduced optineurin expression
- Optineurin knockdown enhances osteoclast differentiation
- Loss of optineurin function increases bone turnover in vivo
- Optineurin inhibits osteoclast formation by modulating NF-κB and IFN-β signaling

Authors

Rami Obaid, Sachin E. Wani, Asim Azfer, ..., Philip Cohen, Stuart H. Ralston, Omar M.E. Albagha

Correspondence

omar.albagha@ed.ac.uk

In Brief

Using mouse models, Obaid et al. identify a role of optineurin in bone metabolism as a negative regulator of osteoclast differentiation. Loss of optineurin function leads to increased bone turnover in mice, suggesting a mechanism by which genetic variants in optineurin predispose to Paget's disease of bone.

Obaid et al., 2015, Cell Reports *13*, 1096–1102
November 10, 2015
http://dx.doi.org/10.1016/j.celrep.2015.09.071

OPEN ACCESS
CellPress

Cell Reports
Report

Optineurin Negatively Regulates Osteoclast Differentiation by Modulating NF-κB and Interferon Signaling: Implications for Paget's Disease

Rami Obaid,[1,4] Sachin E. Wani,[1,4] Asim Azfer,[1] Toby Hurd,[2] Ruth Jones,[3] Philip Cohen,[3] Stuart H. Ralston,[1] and Omar M.E. Albagha[1,*]

[1]Centre for Genomic and Experimental Medicine, Institute of Genetics and Molecular Medicine, University of Edinburgh, Edinburgh EH4 2XU, UK
[2]Medical Research Council Human Genetic Unit, Institute of Genetics and Molecular Medicine, University of Edinburgh, Edinburgh EH4 2XU, UK
[3]Medical Research Council Protein Phosphorylation and Ubiquitylation Unit, The Sir James Black Centre, University of Dundee, Dundee DD1 5HE, UK
[4]Co-first author
*Correspondence: omar.albagha@ed.ac.uk
http://dx.doi.org/10.1016/j.celrep.2015.09.071

SUMMARY

Paget's disease of bone (PDB) is a common disease characterized by osteoclast activation that leads to various skeletal complications. Susceptibility to PDB is mediated by a common variant at the optineurin (OPTN) locus, which is associated with reduced levels of mRNA. However, it is unclear how this leads to the development of PDB. Here, we show that OPTN acts as a negative regulator of osteoclast differentiation in vitro and that mice with a loss-of-function mutation in Optn have increased osteoclast activity and bone turnover. Osteoclasts derived from Optn mutant mice have an increase in NF-κB activation and a reduction in interferon beta expression in response to RANKL when compared to wild-type mice. These studies identify OPTN as a regulator of bone resorption and are consistent with a model whereby genetically determined reductions in OPTN expression predispose to PDB by enhancing osteoclast differentiation.

INTRODUCTION

Paget's disease of bone (PDB) is a common skeletal disorder characterized by osteoclast activation, which provokes increased but disorganized bone turnover, leading to pathological fractures, bone deformity, and bone pain. The disease has a strong genetic component, but the genes responsible have not been fully characterized. The most important predisposing gene is *SQSTM1*, which is mutated in ~10% of patients with the disease. The *SQSTM1* causal mutations increase osteoclastogenesis by enhancing receptor activator of nuclear factor kappa B (NF-κB) (RANK) signaling in osteoclasts and their precursors (Cavey et al., 2006; Daroszewska et al., 2011; Hiruma et al., 2008). Linkage studies in families (Lucas et al., 2008) coupled with genome-wide association studies (GWAS) (Albagha et al., 2010, 2011) have identified a strong susceptibility locus for PDB at the *OPTN* locus on chromosome 10p13. The *OPTN* gene encodes optineurin, a ubiquitously expressed cytoplasmic protein involved in many cellular processes including regulation of NF-κB signaling (Zhu et al., 2007), autophagy, and innate immunity (Wild et al., 2011), but the role of optineurin in bone metabolism is unknown. Here, we investigated the role of OPTN in regulating bone turnover and evaluated the molecular mechanisms by which variants at the *OPTN* locus predispose to PDB.

RESULTS AND DISCUSSION

Reduced Expression of *OPTN* Predisposes to PDB

In order to identify disease-causing mutations in the *OPTN* locus, we conducted mutation screening of the coding exons of *OPTN* in 200 PDB patients, but results showed no mutations in the protein-coding region (data not shown). However, the top GWAS hit (rs1561570) was found to be a strong expression quantitative trait locus (eQTL) in human monocytes (Zeller et al., 2010) and in peripheral blood mononuclear cells (Westra et al., 2013) with substantially reduced levels of *OPTN* mRNA expression in carriers of the PDB-predisposing "T" allele with an evidence of an allele-dose effect (Figure 1). These observations indicate that susceptibility to PDB is associated with reduced expression of *OPTN* and raise the possibility that OPTN might act as a negative regulator of osteoclast function.

Optn Knockdown Enhances Osteoclast Differentiation

Here, we studied the expression of optineurin during osteoclast differentiation and investigated the effects of *Optn* knockdown in primary bone-marrow-derived macrophage (BMDM) cultures. Expression of optineurin increased considerably during osteoclast differentiation, following stimulation of the cultures with macrophage colony-stimulating factor (M-CSF) and receptor

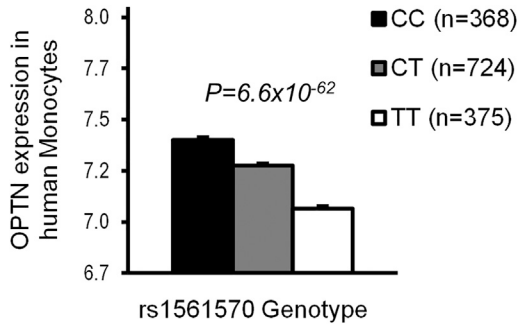

Figure 1. The Paget's-Disease-Associated SNP rs1561570 Is a Strong eQTL in Human Monocytes

OPTN gene expression levels are shown in relation to rs1561570 genotype in human monocytes. The Paget's disease risk allele "T" is associated with reduced *OPTN* gene expression. Data are shown as mean ± SEM; *n* indicates the number of subjects in each genotype group. Data were extracted from (Zeller et al., 2010).

activator of NF-κB ligand (RANKL) (Figure 2A). Knockdown of optineurin by small hairpin RNA (shRNA) in M-CSF- and RANKL-stimulated BMDMs significantly increased osteoclast numbers and size when compared with a non-targeting shRNA control (Figures 2B and 2C). Overexpression of *Optn* in RAW 264 cells resulted in a substantial reduction in the number and size of multinucleated TRAP+ cells formed upon stimulation with RANKL (Figure S1). These experiments illustrate that optineurin acts as a negative regulator of osteoclast differentiation in vitro.

Loss of Optn Function Induces Bone Turnover In Vivo

To investigate the effects of Optn on osteoclast activity and bone remodelling in vivo, we conducted skeletal phenotyping of mice homozygous for a D-to-N amino acid substitution at codon 477 of the optineurin protein ($Optn^{D477N/D477N}$). This is a loss-of-function mutation that encodes a protein that is unable to bind to Lys63-linked ubiquitin chains (Gleason et al., 2011). Bone marrow macrophage cultures from $Optn^{D477N/D477N}$ mice formed significantly more osteoclasts than those from wild-type (WT) littermates and the number of hypernucleated osteoclasts was significantly increased (Figure 3A), replicating exactly the observations in WT cultures subjected to shRNA *Optn* knockdown (Figure 2C). To investigate if Optn affects osteoblast differentiation and/or function, we performed an in vitro bone nodule assay and osteoblast-osteoclast co-culture assays. There was no difference between $Optn^{D477N/D477N}$ and WT mice in the ability of calvarial osteoblasts to form bone nodules in vitro (Figure 3B). However, osteoblast-osteoclast co-culture assays showed that osteoblasts from $Optn^{D477N/D477N}$ mice had reduced ability to support osteoclast differentiation when compared to WT osteoblast cultures (Figure 3C). In contrast, and consistent with bone marrow culture data presented in Figure 3A, osteoclast precursor cells derived from $Optn^{D477N/D477N}$ mice showed enhanced sensitivity to osteoblast stimulation that appears to compensate for the reduction in the ability of mutant osteoblast to support osteoclast differentiation (Figure 3C).

Quantitative bone histomorphometry showed that $Optn^{D477N/D477N}$ mice had significantly increased number of osteoclasts per bone surface (Oc.N/BS) and resorption surfaces (Oc.S/BS) as compared with WT (Figure 3D). Indices of bone formation (osteoid surface per bone surface [OS/BS], osteoid volume per bone volume [OV/BV], and mineral apposition rate [MAR]) were also significantly higher in $Optn^{D477N/D477N}$ mice (Figures 3E and 3F), and there was a non-significant trend ($p = 0.08$) for an increase in bone formation rate (BFR/BS). These observations illustrate that optineurin negatively regulates osteoclast activity both in vitro and in vivo. The lack of an effect on osteoblast differentiation in vitro suggests that the increased bone formation we observed in $Optn^{D477N/D477N}$ in vivo was most probably secondary to the increase in bone resorption, as occurs in humans with PDB (Ralston et al., 2008). Since PDB is also characterized by the development of focal osteolytic lesions that predominantly affect older people, we performed further skeletal phenotyping of $Optn^{D477N/D477N}$ mice to investigate bone mass and bone structure and to look for evidence of focal osteolytic lesions in aged mice using micro-computed tomography (micro-CT) scanning of lower limbs. There was no difference between genotypes in BV/TV, trabecular number, or structure in young mice (Figures S2A and S2B). However, analysis of older mice aged between 8 and 18 months revealed evidence of a focal osteolytic lesion in the left femur in one $Optn^{D477N/D477N}$ mutant mouse aged 15 months (Figure 3G; Table S1). We then investigated the presence of bone lesions in another loss-of-function mouse model in which the C-terminal polyubiquitin-binding domain of Optn has been deleted, resulting in a truncated protein with low expression ($Optn^{\Delta Ex12/\Delta Ex12}$). Analysis of the hindlimbs of $Optn^{\Delta Ex12/\Delta Ex12}$ mice (n = 8) by micro-CT showed no Paget's-disease-like lesions (Table S1). These observations illustrate that while the D477N loss-of-function mutation in Optn increases bone turnover, this does not result in net bone loss, presumably because the increase in bone resorption is coupled with that of bone formation. The development of a focal osteolytic lesion in one $Optn^{D477N/D477N}$ mutant mouse (~10% of mice aged ≥15 months), but not in $Optn^{\Delta Ex12/\Delta Ex12}$, supports the hypothesis that loss of function in optineurin can lead to a PDB-like phenotype while illustrating that additional factors must also be present for focal osteolytic lesions to become fully penetrant.

Optn Regulates Osteoclast Differentiation by Modulating NF-κB and Interferon Signaling

Controlled RANKL-induced NF-κB activation is essential for osteoclast differentiation and function and for the maintenance of normal bone turnover. Previous studies have suggested OPTN as a negative regulator of TNF-α-induced NF-κB activation in immune cells (Maruyama et al., 2010; Nagabhushana et al., 2011; Sudhakar et al., 2009; Zhu et al., 2007), but its role in RANKL-induced NF-κB activation is yet unknown. In order to investigate the effects of Optn on intracellular signaling in osteoclasts, we studied RANKL-induced NF-κB activation during osteoclast differentiation in cultures from $Optn^{D477N/D477N}$ mice as well as in *Optn* knockdown cultures. We found no difference in RANKL-induced NFκB activation, as measured by phosphorylation of IκBα, in BMDMs from D477N mutant mice compared with WT (Figure 4A). However, following RANKL stimulation, there was a progressive increase in NF-κB activation that was

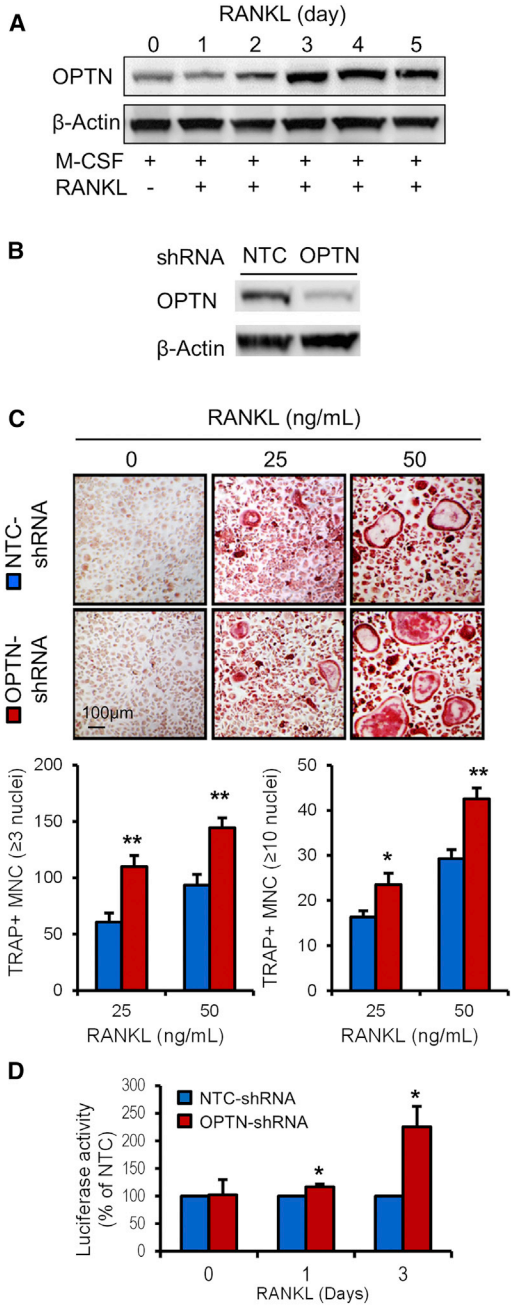

Figure 2. *Optn* Knockdown in Mouse Bone-Marrow-Derived Macrophages Enhances Osteoclast Differentiation

(A) Immunoblot showing the expression of Optn during osteoclast differentiation. BMDMs were stimulated with M-CSF (25 ng/ml) and RANKL (100 ng/ml), and Optn expression was examined in cell lysate at the indicated time points. Anti-β-actin was used as loading control.

(B) Immunoblot showing *Optn* knockdown in BMDMs. Cells were transduced with lentiviral particles expressing shRNA targeting the Optn gene or non-targeting control (NTC).

(C) Enhanced osteoclast differentiation in *Optn* knockdown BMDM. Optn-depleted or NTC cells were stimulated with M-CSF (25 ng/ml) and RANKL (indicated concentrations), and TRAP+ multinucleated cells (MNC) were counted and shown as mean ± SEM from three independent experiments.

(D) RANKL-induced NF-κB activation during osteoclast differentiation. Optn-depleted or NTC cells were transduced with lentiviral particles expressing an NF-κB luciferase reporter followed by stimulation with M-CSF and RANKL, and reporter activity was measured at the indicated time points. Values are mean ± SEM from two independent experiments presented as % of NTC-shRNA. Blots and pictures are representative of three independent experiments. *$p < 0.05$; **$p < 0.01$ compared to NTC.

See also Figure S1.

significantly greater in cultures from $Optn^{D477N/D477N}$ as compared with WT mice, with a maximal effect at 3 days (Figure 4B). Similar findings were observed in *Optn* knockdown cultures in which reduced expression of *Optn* by knockdown resulted in enhanced NF-κB activity after RANKL stimulation (Figure 2D). These findings indicate that the inhibitory effects of *Optn* become most apparent as osteoclast differentiation proceeds and is consistent with the observation that Optn levels increase substantially during osteoclast differentiation (Figure 2A). A similar mechanism has previously been reported in *Cyld* null mice, which show no abnormalities of RANKL-induced NF-κB activation in BMDMs but show enhanced NF-κB activation as osteoclast differentiation proceeds (Jin et al., 2008).

Previous studies have shown that the deubiquitinase enzyme CYLD plays an important negative regulatory role in NF-κB signaling in osteoclasts by interacting with p62 and TRAF6 (Jin et al., 2008). It has also been reported that optineurin is required for CYLD-dependent inhibition of NF-κB activation in immune cells (Nagabhushana et al., 2011). Since the D477N mutation is located in the region that binds to CYLD (Nagabhushana et al., 2011), we studied the effects of the mutant protein on CYLD binding by immunoprecipitation in osteoclasts. This confirmed that the D477N Optn variant had an impaired ability to bind CYLD compared with WT Optn (Figure 4C), indicating that the inhibitory effect of Optn on osteoclast is mediated, in part, by a CYLD-dependent pathway. It has previously been shown that the expression of mutant $Optn^{D477N}$ protein was higher than that of WT in multiple tissues including BMDMs (Gleason et al., 2011). In line with these findings, we also observed that the expression of the mutant $Optn^{D477N}$ protein during osteoclast differentiation was higher than that of the WT (Figures 4C and 4E). This difference was more noticeable from day 3 post-RANKL stimulation (Figure 4E), possibly due to increased NF-κB activity, since a putative NF-κB binding site has been reported in *Optn* promoter (Sudhakar et al., 2009). However, the increased levels of expression of the mutant $Optn^{D477N}$ protein were clearly not sufficient to compensate for its reduced ability to suppress NF-κB activity and osteoclast differentiation.

Studies have shown that while RANKL stimulates osteoclast activity, it also initiates a negative auto-regulatory effect on osteoclasts through induction of interferon beta (IFN-β) expression (Takayanagi et al., 2002; Hayashi et al., 2002), which has an inhibitory effect on osteoclast by interfering with RANKL-induced expression of c-Fos (Takayanagi et al., 2002). Since previous studies have shown that optineurin is involved in IFN-β signaling in immune cells (Gleason et al., 2011; Munitic et al., 2013), we investigated if Optn plays a role in this negative regulatory loop in osteoclast by studying the expression of IFN-β and c-Fos in both WT and $Optn^{D477N/D477N}$ mutant cells. We found

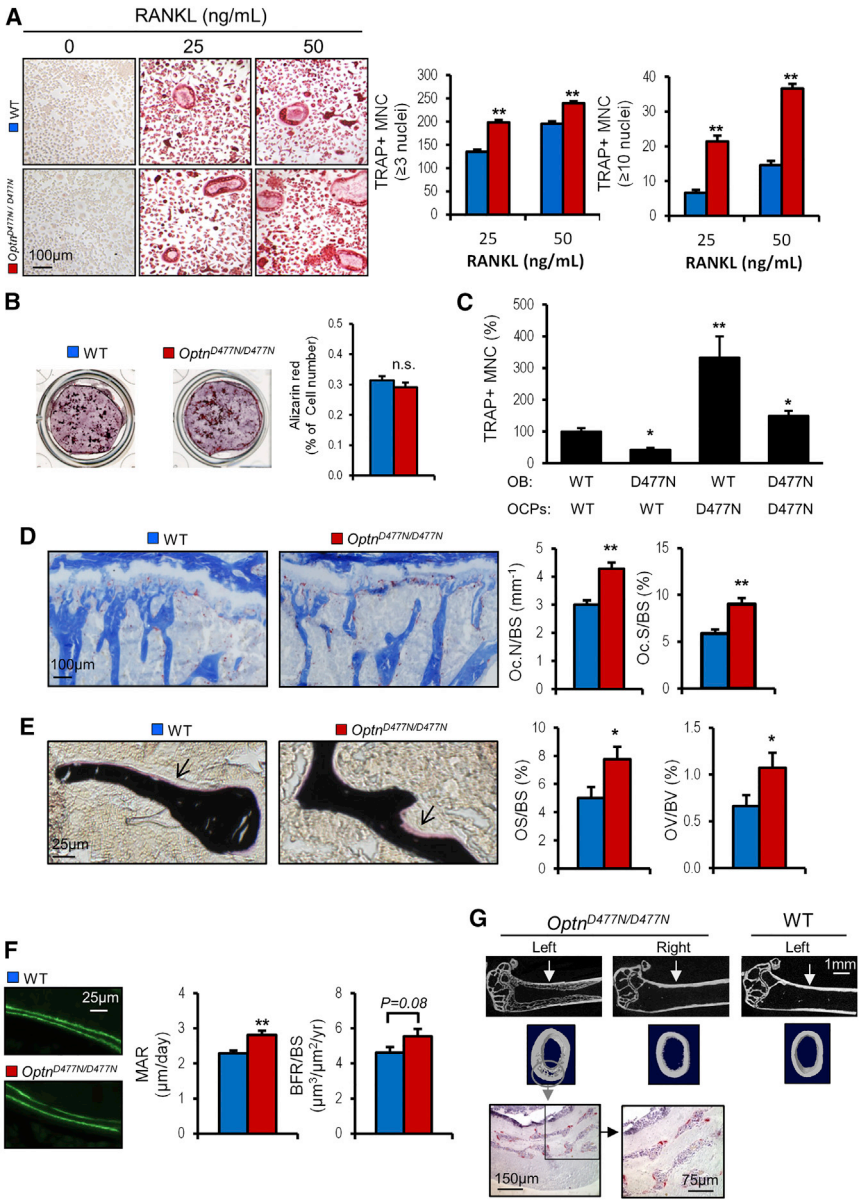

Figure 3. Bone Phenotype of *Optn*$^{D477N/D477N}$ Mice

(A) Enhanced osteoclast differentiation in *Optn*$^{D477N/D477N}$ bone-marrow-derived macrophages (BMDMs). WT and mutant BMDMs were stimulated with M-CSF and RANKL, and the number of TRAP + multinucleated cells (MNC) was counted and shown as mean ± SEM from three independent experiments.

(B) Bone nodule formation assessed by alizarin red staining in neonatal calvarial osteoblasts from WT and *Optn*$^{D477N/D477N}$ mice. Alizarin red values were corrected for viable cell count, and values represent mean ± SEM from three independent experiments.

(C) Osteoblast-osteoclast co-culture assay. Calvarial osteoblasts (OBs) were isolated from WT and *Optn*$^{D477N/D477N}$ mice and co-cultured with bone marrow osteoclast precursor cells (OCPs), and the number of TRAP+ MNC were counted. Values are mean ± SEM from two independent experiments presented as percentage of WT/WT combination.

(D–F) Histomorphometrical analysis of trabecular bone showing enhanced bone turnover in *Optn*$^{D477N/D477N}$ mice. Representative images of proximal tibial metaphysis stained with TRAP (D), Von Kossa (E), or calcein double labeling (F). Graphs on the right represent comparison of bone resorption indices (osteoclast number per bone surface [Oc.N/BS] and osteoclast surface per bone surface [Oc.S/BS]), bone formation indices (osteoid surface per bone surface [OS/BS] and osteoid volume per bone volume [OV/BV]), or dynamic bone formation indices (mineral apposition rate [MAR] and bone formation rate per bone surface [BFR/BS]) between WT and mutant mice. Data are shown as mean ± SEM from seven to eight animals per group.

(G) PDB-like lesions observed in the left femur of a 15-month-old *Optn*$^{D477N/D477N}$ mouse. Micro-CT images showing osteolytic bone lesion within the cortex and histological analysis showing enhanced osteoclastogenesis in the affected region. *p < 0.05, **p < 0.01; n.s., not significant compared to WT.

See also Figure S2 and Table S1.

that RANKL induced the expression of *IFNβ* in both WT and *Optn*$^{D477N/D477N}$ mutant cells, but the expression levels were significantly lower in mutant cells compared to those observed in WT (Figure 4D). Additionally, c-Fos expression during later stages of osteoclast differentiation (3 days post-RANKL stimulation onward) from *Optn*$^{D477N/D477N}$ mice was higher than that observed in WT (Figure 4E). These data suggest that in addition to its inhibitory effect on NF-κB signaling, Optn may also exert an inhibitory role on osteoclast differentiation by modulating the IFN-β signaling pathway.

Coupling between bone formation by osteoblasts and bone resorption by osteoclasts is a complex mechanism, but it is well known that osteoblasts produce many pro-osteoclastogenic cytokines to regulate osteoclast function such as TNFSF11 (RANKL) and IL-6. Expression of these two cytokines in osteoblast cultures derived from *Optn*$^{D477N/D477N}$ mice was significantly lower than that observed in WT cultures, which is consistent with the reduced ability of mutant osteoblast to support osteoclast differentiation (Figures 4F and 4G).

Conclusions

In conclusion, we have demonstrated that reduced expression or loss of Optn function in mice leads to enhanced osteoclast differentiation, identifying Optn as a negative regulator of osteoclast differentiation. The underlying mechanisms are complex but involve RANKL-induced NF-κB activation, an interaction with CYLD, and regulation of IFN-β signaling with regulatory effects that are cell-type specific, dependent on its expression level and on its ability to bind polyubiquitin. Our data

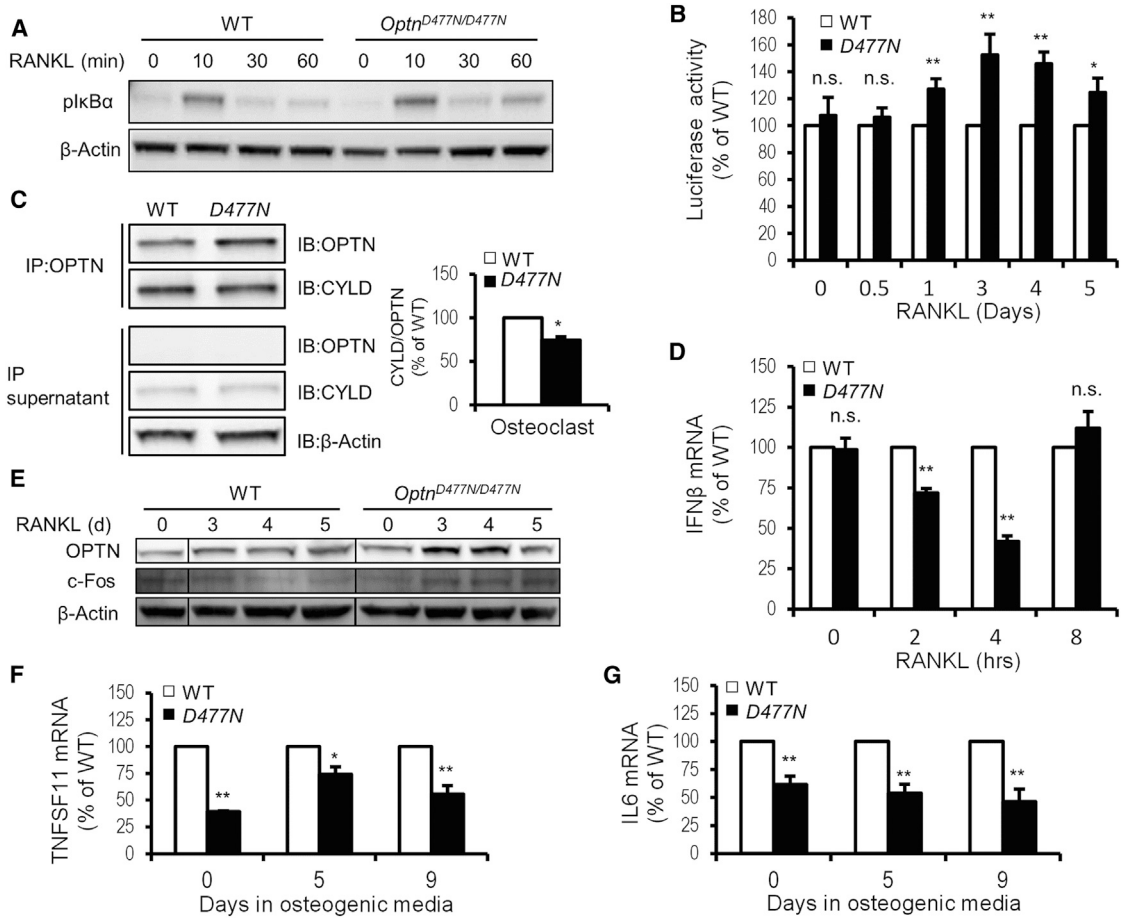

Figure 4. RANKL-Induced NF-κB Activation and IFN-β Induction in *Optn*$^{D477N/D477N}$ Mice

(A) BMDMs from WT or mutant mice were stimulated with RANKL (100 ng/ml) and NF-κB activation was assessed by immunoblotting of pIκBα at the indicated time points.

(B) RANKL-induced NF-κB activation during osteoclast differentiation from WT and mutant mice. BMDMs were transduced with lentiviral particles expressing an NF-κB luciferase reporter followed by stimulation with M-CSF and RANKL, and reporter activity was measured at the indicated time points.

(C) Reduced binding of mutant Optn^{D477N} protein to Cyld in osteoclasts. BMDMs from WT and mutant mice were stimulated with M-CSF and RANKL for 5 days and Optn was immunoprecipitated (IP) from cell lysate, and the presence of Cyld and Optn in the immunoprecipitates was analyzed by immunoblotting (IB). The graph to the right represents band quantification by densitometry of the amount of Cyld in the immunoprecipitates corrected for Optn.

(D) IFN-β mRNA expression in response to RANKL stimulation of WT and *Optn*$^{D477N/D477N}$ osteoclast precursors. Cells were stimulated with RANKL (100 ng/ml), and total RNA was extracted at the indicated time points and analyzed by quantitative real time PCR for IFN-β mRNA levels.

(E) Optn and c-Fos expression during osteoclast differentiation in WT and *Optn*$^{D477N/D477N}$ mice. BMDMs were stimulated with M-CSF (25 ng/ml) and RANKL (100 ng/ml) and expression was assessed by immunoblotting at the indicated time points; lane 1 (WT-0) was rearranged to ease comparison.

(F and G) Expression of *TNFSF11* (F) and IL6 (G) during osteoblast differentiation in WT and *Optn*$^{D477N/D477N}$ mice. Calvarial osteoblasts were isolated and cultured in osteogenic media and mRNA expression was analyzed by quantitative real-time PCR at the indicated time points.

Values in all graphs are mean ± SEM from three independent experiments presented as percentage of WT. mRNA levels were normalized for 18 s rRNA expression, and results are presented as percentage of WT values. *$p < 0.05$, **$p < 0.01$; n.s., not significant compared to WT.

suggest that the common genetic variant rs1561570 at the *OPTN* locus increases susceptibility to PDB by reducing levels of *OPTN* expression, probably leading to enhanced osteoclast differentiation.

EXPERIMENTAL PROCEDURES

Reagents

Details of the materials and reagents can be found in Supplemental Experimental Procedures.

Mice

The generation of *Optn*$^{D477N/D477N}$ knockin mice was described previously (Gleason et al., 2011). To generate *Optn*$^{\Delta Ex12/\Delta Ex12}$, the *Optn*$^{D477N/D477N}$ mice were first crossed to *Flpe*$^{-/-}$ mice to remove the *Flpe* transgene, and these mice were then crossed to *Bal-1 Cre* mice to delete exon 12. All experiments were performed according to institutional, national, and European animal regulations.

Micro-Computed Tomography Analysis

Micro-CT analysis was performed using an in vivo Skyscan 1076 or an ex vivo Skyscan 1172 system. Live animals were scanned on the in vivo scanner

looking for the development of PDB-like lesions as previously described (Daroszewska et al., 2011), and those showing evidence of lesions were further analyzed on the ex vivo scanner and then subjected to histological analysis as described below. Image reconstruction was performed using the Skyscan NRecon package and trabecular bone parameters measured using Skyscan CTAn software.

Histomorphometrical Analysis

Animals received two intraperitoneal injections of calcein 3 days apart before being culled. The hindlimbs were fixed for 24 hr in 4% formalin-buffered saline and stored in 70% ethanol prior to embedding in methyl methacrylate. The bones were processed for static and dynamic histomorphometry according to standard techniques. Sections were stained for tartrate-resistant acid phosphatase (TRAP) with aniline blue counterstain to visualize osteoclasts and osteoid analysis was done after Von Kossa staining with Van Gieson counterstaining according to standard protocols as previously described (Erben and Glösmann, 2012). Histomorphometry was performed using custom-built software and followed standardized nomenclature and recommendations (Dempster et al., 2013).

Osteoclast Culture

Bone marrow cells were isolated from the long bones of 4-month-old mice and cultured for 48 hr in the presence of M-CSF (100 ng/ml) to generate BMDMs. Adherent cells were reseeded and stimulated with M-CSF (25 ng/ml) and RANKL for 5 days until osteoclasts were formed. Cells were fixed with 4% (v/v) formaldehyde in PBS and stained for TRAP. TRAP-positive multinucleated osteoclasts (more than three nuclei) were counted, and numbers were compared to the WT control. For the NF-κB activation assay, BMDMs were generated as described above and incubated under standard conditions for 24 hr. Cells were serum starved for 1 hr followed by stimulation with 100 ng/ml RANKL. Cell lysates were collected at different time points and assayed by immunoblotting. For the NF-κB luciferase reporter assay, BMDMs were transduced with lentiviral NF-κB luciferase reporter for 2 days followed by selection for 48 hr using puromycin (5 μg/ml). The cells were then plated in 96-well plates and luciferase activity was measured with a SteadyGlo-luciferase reporter assay system at the indicated time points following M-CSF (25 ng/ml) and RANKL stimulation (100 ng/ml) using a Bio-Tek Synergy HT plate reader. The medium used was complete minimum essential medium alpha modification (αMEM), and all cultures were incubated under standard conditions of 5% CO_2 and 37°C in a humidified atmosphere.

Osteoblast Culture and Bone Nodule Assay

Osteoblasts were isolated from the calvarial bones of 2-day-old mice by sequential collagenase/EDTA digestion and cultured in complete αMEM medium. On reaching confluence, cells were detached with trypsin, re-plated in 12-well plates at a density of 1×10^5 cells/well, and cultured in osteogenic medium (complete αMEM supplemented with 50 μg/ml vitamin C and 3 mM β-glycerophosphate). The medium was replaced three times per week, and cultures were continued for up to 21 days. Mineralized nodules were detected using alizarin red staining, and bone nodule formation was quantified by destaining the cultures in 10% (w/v) cetylpyridinium chloride and dissolving the stain in 10 mM sodium phosphate (pH 7.0). The absorbance of the extracted stain was then measured at 562 nm and compared to an alizarin red standard curve. Alizarin red values were corrected for viable cell number as determined by the alamar blue assay.

Optn Knockdown

Bone marrow cells from WT mice were isolated and cultured for 48 hr in complete αMEM supplemented with M-CSF (100 ng/ml). The adherent BMDMs were then transduced with either lentiviral particles containing shRNA targeted against the *Optn* gene or negative control particles (non-targeting lentiviral particles). Transduced cells were selected for 48 hr using puromycin (5 μg/ml). Optn-depleted BMDMs were then plated in 96-well plates and stimulated with M-CSF (25 ng/ml) and RANKL (25 or 50 ng/ml) until osteoclasts were formed. TRAP-positive multinucleated osteoclasts were counted and numbers were compared to the non-targeted negative control. Optn-depletion was confirmed at all stages of osteoclast differentiation by immunoblotting.

Statistical Analyses

Values in the graphs indicate group means ± SEM, as indicated in the legends. Comparisons between groups were performed by two-tailed t test. $p < 0.05$ was considered to indicate statistical significance. Experiments were performed as independent replicates as indicated in figure legends.

SUPPLEMENTAL INFORMATION

Supplemental information includes Supplemental Experimental Procedures, two figures, and one table and can be found with this article online at http://dx.doi.org/10.1016/j.celrep.2015.09.071.

AUTHOR CONTRIBUTIONS

R.O. and S.E.W. performed the majority of the experiments with participation from A.A. and R.J. T.H. contributed to *Optn* overexpression experiments. P.C. provided the $Optn^{D477N}$ and $Optn^{\Delta Ex12}$ mice and contributed to study design. S.H.R contributed to study design and paper writing. O.M.E.A. designed and supervised the whole project and wrote the paper.

ACKNOWLEDGMENTS

We thank Rob van 't Hof for help in bone histomorphometry and micro-CT, Antonia Sophocleous and Euphemie Landao-Basonga for assistance in histology, and Catherine Gleason for initial work related to this project. This study was supported mainly by a consolidator grant from the European Research Council to O.M.E.A. (311723-GENEPAD) and by grants from Arthritis Research UK to S.H.R. and O.M.E.A. (19799 and 19520).

Received: November 12, 2014
Revised: September 8, 2015
Accepted: September 24, 2015
Published: October 29, 2015

REFERENCES

Albagha, O.M., Visconti, M.R., Alonso, N., Langston, A.L., Cundy, T., Dargie, R., Dunlop, M.G., Fraser, W.D., Hooper, M.J., Isaia, G., et al. (2010). Genome-wide association study identifies variants at CSF1, OPTN and TNFRSF11A as genetic risk factors for Paget's disease of bone. Nat. Genet. *42*, 520–524.

Albagha, O.M., Wani, S.E., Visconti, M.R., Alonso, N., Goodman, K., Brandi, M.L., Cundy, T., Chung, P.Y., Dargie, R., Devogelaer, J.P., et al.; Genetic Determinants of Paget's Disease (GDPD) Consortium (2011). Genome-wide association identifies three new susceptibility loci for Paget's disease of bone. Nat. Genet. *43*, 685–689.

Cavey, J.R., Ralston, S.H., Sheppard, P.W., Ciani, B., Gallagher, T.R., Long, J.E., Searle, M.S., and Layfield, R. (2006). Loss of ubiquitin binding is a unifying mechanism by which mutations of SQSTM1 cause Paget's disease of bone. Calcif. Tissue Int. *78*, 271–277.

Daroszewska, A., van 't Hof, R.J., Rojas, J.A., Layfield, R., Landao-Basonga, E., Rose, L., Rose, K., and Ralston, S.H. (2011). A point mutation in the ubiquitin-associated domain of SQSMT1 is sufficient to cause a Paget's disease-like disorder in mice. Hum. Mol. Genet. *20*, 2734–2744.

Dempster, D.W., Compston, J.E., Drezner, M.K., Glorieux, F.H., Kanis, J.A., Malluche, H., Meunier, P.J., Ott, S.M., Recker, R.R., and Parfitt, A.M. (2013). Standardized nomenclature, symbols, and units for bone histomorphometry: a 2012 update of the report of the ASBMR Histomorphometry Nomenclature Committee. J. Bone Miner. Res. *28*, 2–17.

Erben, R.G., and Glösmann, M. (2012). Histomorphometry in rodents. Methods Mol. Biol. *816*, 279–303.

Gleason, C.E., Ordureau, A., Gourlay, R., Arthur, J.S., and Cohen, P. (2011). Polyubiquitin binding to optineurin is required for optimal activation of TANK-binding kinase 1 and production of interferon β. J. Biol. Chem. *286*, 35663–35674.

Hayashi, T., Kaneda, T., Toyama, Y., Kumegawa, M., and Hakeda, Y. (2002). Regulation of receptor activator of NF-kappa B ligand-induced osteoclastogenesis by endogenous interferon-beta (INF-beta) and suppressors of cytokine signaling (SOCS). The possible counteracting role of SOCSs- in IFN-beta-inhibited osteoclast formation. J. Biol. Chem. *277*, 27880–27886.

Hiruma, Y., Kurihara, N., Subler, M.A., Zhou, H., Boykin, C.S., Zhang, H., Ishizuka, S., Dempster, D.W., Roodman, G.D., and Windle, J.J. (2008). A SQSTM1/p62 mutation linked to Paget's disease increases the osteoclastogenic potential of the bone microenvironment. Hum. Mol. Genet. *17*, 3708–3719.

Jin, W., Chang, M., Paul, E.M., Babu, G., Lee, A.J., Reiley, W., Wright, A., Zhang, M., You, J., and Sun, S.C. (2008). Deubiquitinating enzyme CYLD negatively regulates RANK signaling and osteoclastogenesis in mice. J. Clin. Invest. *118*, 1858–1866.

Lucas, G.J., Riches, P.L., Hocking, L.J., Cundy, T., Nicholson, G.C., Walsh, J.P., and Ralston, S.H. (2008). Identification of a major locus for Paget's disease on chromosome 10p13 in families of British descent. J. Bone Miner. Res. *23*, 58–63.

Maruyama, H., Morino, H., Ito, H., Izumi, Y., Kato, H., Watanabe, Y., Kinoshita, Y., Kamada, M., Nodera, H., Suzuki, H., et al. (2010). Mutations of optineurin in amyotrophic lateral sclerosis. Nature *465*, 223–226.

Munitic, I., Giardino Torchia, M.L., Meena, N.P., Zhu, G., Li, C.C., and Ashwell, J.D. (2013). Optineurin insufficiency impairs IRF3 but not NF-κB activation in immune cells. J. Immunol. *191*, 6231–6240.

Nagabhushana, A., Bansal, M., and Swarup, G. (2011). Optineurin is required for CYLD-dependent inhibition of TNFα-induced NF-κB activation. PLoS ONE *6*, e17477.

Ralston, S.H., Langston, A.L., and Reid, I.R. (2008). Pathogenesis and management of Paget's disease of bone. Lancet *372*, 155–163.

Sudhakar, C., Nagabhushana, A., Jain, N., and Swarup, G. (2009). NF-kappaB mediates tumor necrosis factor alpha-induced expression of optineurin, a negative regulator of NF-kappaB. PLoS ONE *4*, e5114.

Takayanagi, H., Kim, S., Matsuo, K., Suzuki, H., Suzuki, T., Sato, K., Yokochi, T., Oda, H., Nakamura, K., Ida, N., et al. (2002). RANKL maintains bone homeostasis through c-Fos-dependent induction of interferon-beta. Nature *416*, 744–749.

Westra, H.J., Peters, M.J., Esko, T., Yaghootkar, H., Schurmann, C., Kettunen, J., Christiansen, M.W., Fairfax, B.P., Schramm, K., Powell, J.E., et al. (2013). Systematic identification of trans eQTLs as putative drivers of known disease associations. Nat. Genet. *45*, 1238–1243.

Wild, P., Farhan, H., McEwan, D.G., Wagner, S., Rogov, V.V., Brady, N.R., Richter, B., Korac, J., Waidmann, O., Choudhary, C., et al. (2011). Phosphorylation of the autophagy receptor optineurin restricts Salmonella growth. Science *333*, 228–233.

Zeller, T., Wild, P., Szymczak, S., Rotival, M., Schillert, A., Castagne, R., Maouche, S., Germain, M., Lackner, K., Rossmann, H., et al. (2010). Genetics and beyond–the transcriptome of human monocytes and disease susceptibility. PLoS ONE *5*, e10693.

Zhu, G., Wu, C.J., Zhao, Y., and Ashwell, J.D. (2007). Optineurin negatively regulates TNFalpha- induced NF-kappaB activation by competing with NEMO for ubiquitinated RIP. Curr. Biol. *17*, 1438–1443.

Cell Reports

Supplemental Information

Optineurin Negatively Regulates Osteoclast Differentiation by Modulating NF-κB and Interferon Signaling: Implications for Paget's Disease

Rami Obaid, Sachin E. Wani, Asim Azfer, Toby Hurd, Ruth Jones, Philip Cohen, Stuart H. Ralston, and Omar M.E. Albagha

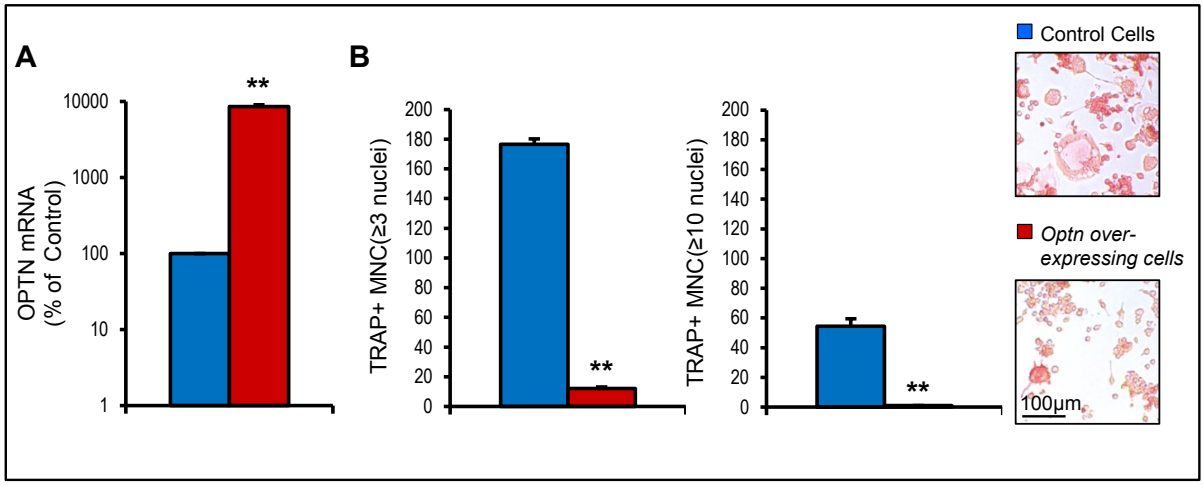

Figure S1. Overexpression of *Optn* in RAW Cells Reduces their Ability to Form TRAP+ Multinucleated (MNC) Cells Upon Stimulation with RANKL, Related to figure 2. (**A**) *Optn* mRNA expression in cells overexpressing *Optn* (red bar) compared to control cells (blue bar). mRNA levels were assayed by qRT-PCR and normalised for 18s rRNA and presented as % of control cells. (**B**) The number of TRAP+ MNC (≥3 nuclei) or hypernucleated MNC (≥10 nuclei) generated from RAW cells overexpressing *Optn* compared to control cells. Values are means ± SEM representative from two-three independent experiments. ** P< 0.01.

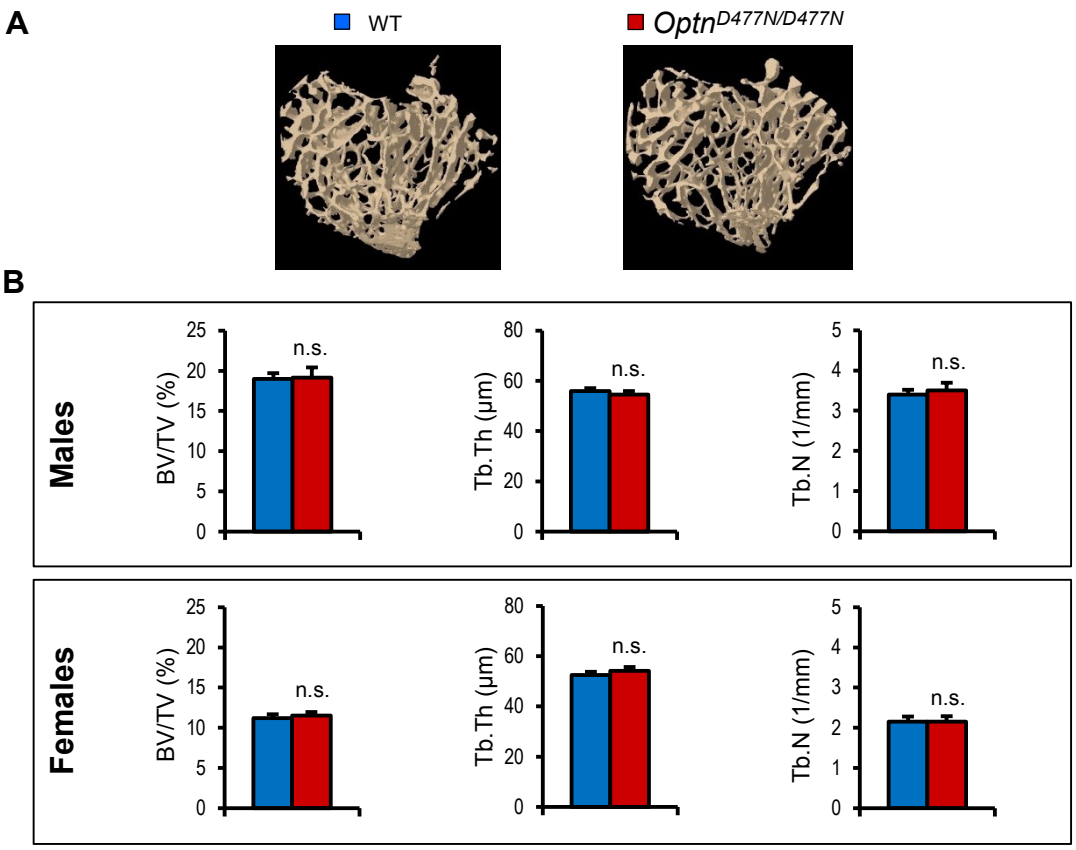

Figure S2. Analysis of Bone Structure in *Optn*$^{D477N/D477N}$ Mice by MicroCT, Related to figure 3. (**A**) Representative MicroCT images of trabecular bone from the tibial metaphysis of *Optn*$^{D477N/D477N}$ and WT mice. (**B**) Comparison of bone volume/total volume (BV/TV); trabecular thickness (Tb.Th) and trabecular number (Tb.N) between WT and mutant male and female mice. Values are means ± SEM from eight mice per group. n.s.; not significant.

Table S1. WT, *Optn*$^{D477N/D477N}$, and *Optn*$^{\Delta Ex12/\Delta Ex12}$ Mice Screened for the Presence of PDB-Like Lesions by MicroCT, Related to figure 3.

Mouse Model	*Optn*$^{D477N/D477N}$									*Optn*$^{\Delta Ex12/\Delta Ex12}$	
Age group	8-9 months			12 months			15-18 months			7-12 months	
Genotype	WT	D477N		WT	D477N		WT	D477N		WT	ΔEx12
Males (*n*)	7	11		8	12		2	6		3	4
Females (*n*)	13	7		12	13		6	3		4	4
Total (*n*)	20	18		20	25		8	9		7	8
Male with lesion (*n*)	0	0		0	0		0	0		0	0
Female with lesion (*n*)	0	0		0	0		0	1		0	0
Total with lesion (*n*)	0	0		0	0		0	1		0	0

Supplemental Experimental Procedures

Reagents:

Cells: RAW 264.7 (ATCC). *Media*: Minimal Essential Medium Eagle alpha modification (α-MEM; Sigma), Fetal Calf Serum (FCS; Hyclone) and L-Glutamine (Invitrogen). The complete α-MEM medium consisted of α-MEM supplemented with 10% fetal calf serum, 2 mM L-glutamine, 100 U/ml penicillin, and 100 µg/ml streptomycin. *Antibodies*: OPTN (1:250, Cayman), c-Fos (1:100, Calbiochem), Actin (1:1000, Sigma), Phospho-IκBα (Ser32; 1:1000 Cell Signalling) and CYLD (1:1000, Cell Signalling). *Cytokines*: Murine M-CSF (Prospec Tech.) and human recombinant RANK-L (gift from Dr. Patrick Mollat-Proskelia SASU). *Other reagents:* Protein G-agarose (Calbiochem), puromycin (GIBCO), penicillin; streptomycin; and Alamar blue (Invitrogen), geneticin (Neomycin analogue-G418; Life Technology), Alizarin red; cetylpyridinium chloride; calcein; vitamin C; and β glycerophosphate (Sigma). *Kits*: Cignal Lenti NF-κB reporter (SA Biosciences), Mission mouse *Optn* shRNA pLKO.1-puro clones (Sigma), Trans-lentiviral packaging kit (Thermo Scientific), GenEZ ORF clone for *Mus musculus* Optineurin (OMu13999; Genscript), GenElute Mammalian Total RNA kit (Sigma), qScript cDNA SuperMix kit (QuantaBioscience), SensiFAST Probe No-ROX kit (Bioline), Steady Glo Luciferase Assay (Promega) and jetPEI-Macrophage transfection reagent (Polyplus Transfection).

Osteoblast-Osteoclast Co-culture Assay

Osteoblastic cells (5 x 10^4 cells per well) isolated from the calvariae of 7-10 week old mice by sequential collagenase/EDTA digestion were co-cultured with bone marrow cells (5 X 10^5 cells per well) in a 24-well plate in α-MEM supplemented with 2 mM L-glutamine, 100 U/ml penicillin, 100 µg/ml streptomycin, 10% Heat inactivated FCS and 10 nM 1α,25$(OH)_2$ D3. The culture medium was replaced every 2-3 days and cells were fixed after 8 days, TRAP stained and TRAP positive multinucleated osteoclasts were counted.

Immunoblotting and Immunoprecipitation

Cells were lysed using RIPA buffer and cell lysates were subjected to sodium dodecyl sulphate polyacrylamide gel electrophoresis (SDS-PAGE) and electroblotted onto Hybond-P (Amersham) membranes. Membranes were blocked with 5% (w/v) non-fat milk in Tris buffered saline with TBS-tween (50 mM Tris, 150 mM NaCl, 0.1%

[v/v] Tween-20) and probed with rabbit primary antibodies. After washing with TBST, membranes were incubated with anti-rabbit horseradish peroxidise conjugated secondary antibody (1:5000) washed and visualized using SuperSignal West Dura Extended Duration Substrate (Thermo Scientific) on a SynGene GeneGnome/ Licor imager. Intensities of bands were quantified using SynGene Gene Tools software/ Image Studio Lite Ver 3.1 software.

To immunoprecipitate OPTN, 50 µg of cell extract protein was incubated overnight at 4°C with 4 µg of sheep anti-mouse Optn antibody (s308c). After rotation overnight at 4°C with 15 µl protein G-agarose, the beads were collected by centrifugation, washed three times with modified RIPA buffer, denatured and subjected to SDS-PAGE, and immunoblotted as mentioned above.

Optn Overexpression

RAW cells were seeded at a density of 1.5 million cells per T25 and transfected with GenEZ *Optn* ORF expression plasmid using jetPEI according to the manufacturer protocol. A stable line of *Optn* overexpressing cells was generated following 3 weeks of selection using 400 ug/ml neomycin. Overexpression was confirmed by qRT-PCR. Cells overexpressing *Optn* or control cells were seeded in 96-well plate (5000/well) in Dulbecco's Modified Eagle's Medium (DMEM; Sigma) and stimulated with RANKL (100 ng/ml) for 4 days. Cells were then fixed, TRAP stained and TRAP positive multinucleated cells were counted.

Quantitative Real-Time PCR (qRT-PCR)

Total RNA was isolated using GenElute Mammalian Total RNA Kit and RNA was quantified using the Nanodrop 1000 Spectrophotometer. Complementary DNA was generated by RT-PCR using the qScript cDNA SuperMix kit following the manufacturer's instructions. Primers and labelled probes were designed using the Primer 3 and the Roche Diagnostics website (Roche). The primer sequences were as follows: IFNB1-F, 5'-cacagccctctccatcaacta-3', IFNB1-R, 5'-catttccgaatgttcgtcct-3', TNFSF11-F, 5'-tgaagacacactacctgactcctg-3', TNFSF11-R, 5'-ccacaatgtgttgcagttcc-3', IL6-F, 5'-gctaccaaactggatataatcagga-3', IL6-R, 5'-ccaggtagctatggtactccagaa-3', OPTN-F, 5'-gctccgaaatcaagatggag-3', and OPTN-R, 5'-gcagagtggctaacctggac-3'. Real-time PCR was performed using SensiFAST Probe No-ROX kit on a Chromo 4TM Detector and quantified using the Opticon MonitorTM software version 3.1.

Samples were normalized to 18s rRNA expression. 18s cDNA was amplified with the VIC-labelled predesigned probe-primer combination from Applied Biosystems (4319413E) allowing two channel detection of one cDNA.